

## Photoacoustic-spectra studies on $\text{BaX}_2:\text{Eu}^{2+}$ ( $X = \text{F, Cl, Br}$ ) phosphors

Zhang Yugeng

Department of Applied Chemistry, University of Science and Technology of China, Hefei, Anhui, 230026, People's Republic of China

(Received 22 April 1994; revised manuscript received 5 December 1994)

The photoacoustic (PA) technique was used to study the properties of storage phosphors. The optical properties, excited-state energy levels, the deexcitation processes, and the properties of F centers were studied systematically. The PA properties of  $\text{BaFBr}:\text{Eu}^{2+}$ ,  $\text{BaFCl}:\text{Eu}^{2+}$ , and  $\text{BaCl}_2:\text{Eu}^{2+}$  were discussed in this work. As to the PA spectra, the emission efficiency of  $4f^65d^1 \rightarrow 4f^7$  are larger than that of  $4f^7 \rightarrow 4f^7$  deexcitation process in these materials. In addition, within the photostimulable luminescence deexcitation process there exist some fast nonradiative deexcitation processes, which support the model of Von Seggern.

### I. INTRODUCTION

Prompt and delayed luminescence from inorganic phosphors as a result of x-ray irradiation has been studied for many decades.<sup>1-3</sup> Recently a class of phosphors ( $\text{Eu}^{2+}$ -doped alkali-earth halides) has been introduced which is able to store x-ray information for hours and allows a recovery of this information by optical stimulation within microseconds. The alkali-earth halide  $\text{BaX}_2:\text{Eu}^{2+}$  ( $X = \text{F, Cl, Br}$ ) presently shows the most promising properties when commercially used in x-ray storage films. In publications by a number of authors, properties of the materials have been reported.<sup>4-6</sup> Additionally, image quality factors of actual x-ray films utilizing  $\text{BaFBr}:\text{Eu}$  have been measured.<sup>7,8</sup> The optical properties, dynamic models, and some other properties of these materials have been widely studied.<sup>9,10</sup> But, some problems also exist that must be resolved. Although the optical properties of these materials are widely studied, the studying of excited-state energy levels and the deexcitation processes are limited and confused. The disputation has also existed between Takahashi and Von Seggern with the photostimulable luminescence (PSL) kinetic process model for many years. In this paper, the advantage of the photoacoustic (PA) technique is used to study these problems. With the PA technique, the emission efficiency of different deexcitation processes and that of different phosphors materials are studied, especially by the phase shift of the PA spectrum. However, the photoacoustic spectra properties of these phosphors have been studied in a very limited way.<sup>11</sup> The PA technique, in fact, is a very useful method in studying the properties of this kind of material.

Recently, the photoacoustic measurement has been widely used to investigate the physical and chemical properties of many kinds of samples.<sup>12,13</sup> The PA spectroscopy enables one to obtain spectra on any type of solid, whether it is crystalline, powder, or gel, and whether it is a direct monitor of energy gap and the nonradiative deexcitation process, the complement of absorption and photoluminescence spectroscopy.<sup>14</sup>

The PA effect is selectively sensitive only to the heat-producing deexcitation processes that take place in the

sample after the absorption of modulated light. In general, apart from the thermal deexcitation channel, several other deexcitation channels, such as fluorescence, photochemistry, photoconductivity, etc., are simultaneously competing with each other. Denoting by  $E^0$  the energy absorbed by a given system, the heat produced can be expressed as

$$Q = E^0 \left[ 1 - \sum \gamma_i \right], \quad (1)$$

where the  $\gamma_i$  are the conversion efficiencies of several nonthermal deexcitation channels. Since the PA signal is proportional to  $Q$ , it can, in general, be written as

$$S = S^0 \left[ 1 - \sum \gamma_i \right], \quad (2)$$

where  $S^0$  represents the PA signal if only the thermal deexcitation channel is active. Equation (2) tells us that the PA signal is complementary to the other photoinduced energy conversion processes. That is, when an optically excited energy level of a given system decays by means, say, of fluorescence or undergoes a photochemical reaction, then little or no acoustic signal is produced.

In PA theory, the phase shift of the PA spectrum is connected with the time of deexcitation process of respective excited energy levels. The time delay may be calculated from the phase angle  $\phi$  by<sup>15</sup>

$$\tau = \text{tg } \phi / (2\pi f), \quad (3)$$

where  $f$  is the modulated frequency.

According this idea, the optical properties, the excited-state energy levels, the deexcitation processes and the properties of the F center are studied on  $\text{BaX}_2:\text{Eu}^{2+}$  ( $X = \text{F, Cl, Br}$ ) materials.

### II. EXPERIMENT

The materials  $\text{BaFBr}:\text{Eu}^{2+}$ ,  $\text{BaFCl}:\text{Eu}^{2+}$ ,  $\text{BaCl}_2:\text{Eu}^{2+}$  were prepared by mixing  $\text{BaFBr}$ ,  $\text{BaFCl}$ ,  $\text{BaCl}_2$  with  $\text{EuO}$  and ground, then sintering in a quartz tube furnace as the gas  $\text{N}_2$  was introduced. In the measurement of PA spectra, the excitation source a 500 W xenon lamp and the optical system was a CT-30F monochromator combined

with an appropriate absorption filter to eliminate multiple-order effects. The light source was modulated by a variable-speed mechanical chopper at a certain frequency, 12 Hz. The acoustic signal was detected with the sample placed in a locally built photoacoustic cell fitted with an ERM-10 electret microphone. After preamplification, the output of the microphone was fed to a lock-in amplifier (LI-574A) to which a reference signal was input from the chopper. The output signal was normalized for changes in lamp intensity using a carbon-black reference.

### III. RESULTS AND DISCUSSION

#### A. The PA spectrum of BaFBr:Eu<sup>2+</sup>

Figure 1 shows the absorption spectrum (ABS), the excitation spectrum (EXS), and the PA spectrum (PAS) of the BaFBr:Eu<sup>2+</sup> material. It is seen that the absorption spectrum has an absorption band at 250–320 nm. The excitation spectrum of the Eu<sup>2+</sup> luminescence has a peak at 280 nm and the PA spectrum has a signal band at 250–300 nm. It is seen that the excitation spectrum and the PA spectrum are corresponding to the absorption spectrum. As seen in Eq. (1),  $\gamma_i$  is the conversion efficiency of fluorescence deexcitation process in this material and it is sensitively shown in the excitation spectrum. The PA effect is selectively sensitive only to the nonradiative deexcitation processes and the PA signal is written as Eq. (2). So, the PA spectrum and the excitation spectrum are the complement of the absorption spectrum. According to this, the emission efficiency can be studied by the PA spectrum.

The PA amplitude spectrum and the PA phase spectra are shown in Fig. 2. There, two linear spectrum peaks are observed at 250 and 263 nm, and another wide band spectrum peak is observed at 280–400 nm. However, the linear peaks originate from the deexcitation processes of  $f \rightarrow f$  and the band peak is due to the deexcitation process of  $4f^65d^1 \rightarrow 4f^7$ , see Fig. 3. Comparing to the absorption spectrum, the relative intensity of linear

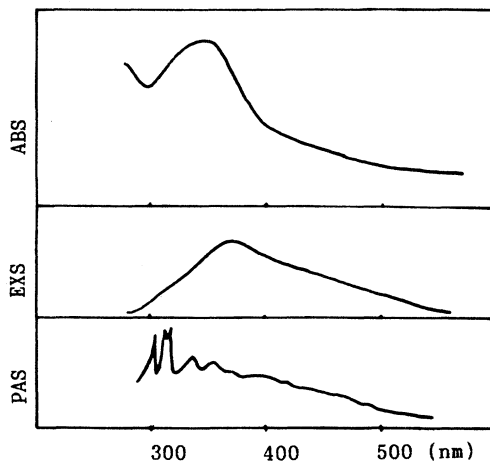


FIG. 1. Spectra for the excitation process in BaFBr:Eu<sup>2+</sup>.

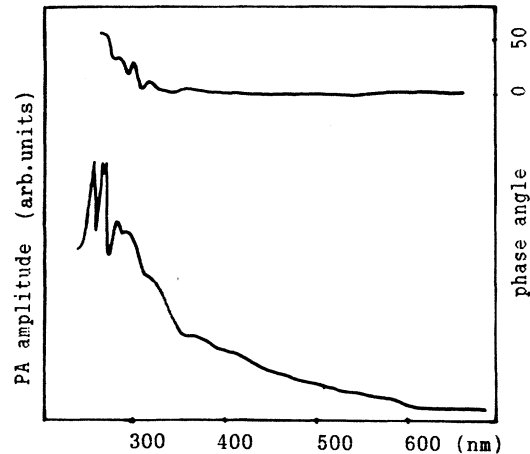


FIG. 2. The PA amplitude and phase spectra of BaFBr:Eu<sup>2+</sup>.

peaks is much larger than that of band peak. It is said that the emission efficiency of the deexcitation channel  $4f^65d^1 \rightarrow 4f^7$  is much larger than that of the  $4f^7 \rightarrow 4f^7$  deexcitation process. As seen in Fig. 3, the nonradiative deexcitation processes of linear peaks at 250 and 263 nm are between the different excited-state energy levels. As to band peak in Fig. 2, the PA signal intensity of the high-energy edge is larger than that of low-energy edge. This is also due to the deexcitation process between  $e_g$  and  $t_{2g}$  ( $4f^65d^1$ ) and their splitting energy levels.

The PA phase spectrum is also shown in Fig. 2. It is seen that the different deexcitation processes have different phase shifts. With the phase angle, the time ( $\tau$ ) of the deexcitation process is calculated by Eq. (3), where the time delay ( $\tau$ ) of the rare-earth ion is mostly defined by the life of the excited state of Eu<sup>2+</sup>. This is an important parameter for us to study the deexcitation processes of phosphor materials. The transfer properties of the deexcitation process may be determined by their respective time delay ( $\tau$ ). In the PA measurement of this work, the scan speed is 60 nm/sec. So, since the phase angle is larger than 50°, the phase spectrum will be very complex and difficult to interpret. In Fig. 2, the phase angle of the linear peak at 250 nm is larger than 50°, and its deexcita-

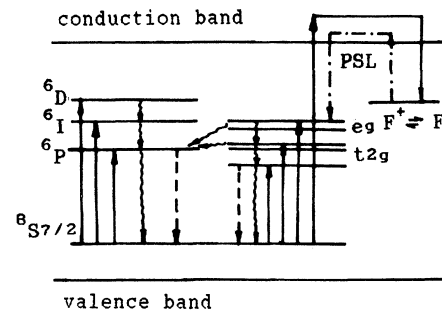


FIG. 3. Energy term scheme of BaFBr:Eu<sup>2+</sup>.  $\longrightarrow$ , the excitation process;  $\rightsquigarrow$ , nonradiative process;  $\dashrightarrow$ , radiative process;  $\dashrightarrow$ , PSL process.

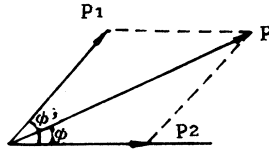


FIG. 4. The relations of the PA signal occurred in one range produced by different deexcitation processes.

tion time is larger than 15.8 msec. The phase angle of linear peak at 263 nm is  $50^\circ$  and its deexcitation time is calculated as 15.8 msec. It is said that the deexcitation processes of  $4f^7 \rightarrow 4f^7$  are slow processes and the lifetime of the excited state  $4f^7$  is quite long. Besides several weak peaks observed at the high-energy edge, the phase shifts of the  $4f^6 5d^1 \rightarrow 4f^7$  deexcitation processes are very small, nearly zero. It is seen that this deexcitation channel is a very fast process with a delay time smaller than the  $\mu\text{sec}$  range, and the weak peaks shown in the phase spectrum are due to the deexcitation processes of  ${}^6P_{7/2} \rightarrow {}^8S_{7/2}$  or  $e_g(t_{2g}) \rightarrow {}^6P_{7/2} \rightarrow {}^8S_{7/2}$ , see Fig. 3 and Table I. They are the slow processes with weak intensity and are also shown in the PA amplitude spectrum. According to the PA amplitude spectrum, we find that the PA signal of slow processes in the range 270–400 nm is overlapped with the PA signal of the fast deexcitation processes introduced above (with weak intensity). So, the phase angles of the slow deexcitation processes  $\phi'$  must be resolved as

$$\phi' = \arcsin \left( \frac{P}{P^1} \sin \phi \right), \quad (4)$$

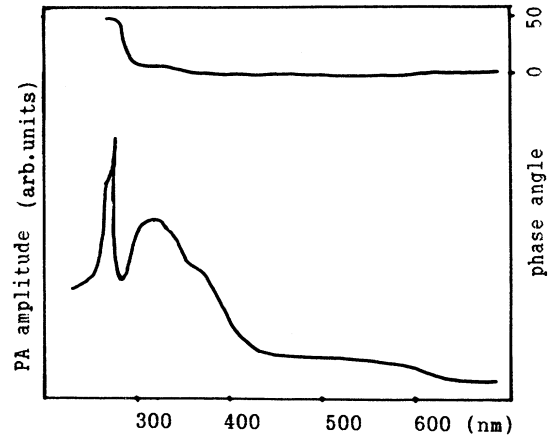


FIG. 5. The PA amplitude and phase spectrum of  $\text{BaFCl:Eu}^{2+}$ .

where  $P$  and  $\phi$  are the observed amplitude and phase angle of the PA signal,  $P^1$  is the PA amplitude of the slow deexcitation process, see Fig. 4. In Fig. 4,  $P^2$  is the PA amplitude of the fast deexcitation process. By this method, the time of the deexcitation process is calculated and presented in Table I.

However, there exists a weak PA signal in the range 400–600 nm. This is the photostimurable luminescence (PSL) deexcitation process as the sample was exposed by UV light.<sup>4</sup> It is said that the PSL process also has some nonradiative deexcitation process and can be monitored by the PA technique. The phase shift of the PSL

TABLE I. The PA spectra (nm) and deexcitation processes of  $\text{BaX}_2\cdot\text{Eu}^{2+}$  ( $X=\text{F,Br,Cl}$ ) materials.

$\text{BaX}_2\cdot\text{Eu}$	Obs.	PA band <sup>a</sup>	Deexcitation process	Phase	Time delay
$\text{BaFBr:Eu}$	250	<i>L, S</i>	${}^6D_{7/2} \rightarrow {}^6P_{7/2} \rightarrow {}^8S_{7/2}$	$> 50^\circ$	$> 15.8$ msec
	262	<i>L, S</i>	${}^6I_{7/2} \rightarrow {}^6P_{7/2} \rightarrow {}^8S_{7/2}$	$50^\circ$	15.8 msec
	264	<i>L, S</i>	$e_g \rightarrow {}^6P_{7/2} \rightarrow {}^8S_{7/2}$	$50^\circ$	15.8 msec
	281	<i>L, W</i>	$t_{2g} \rightarrow {}^6P_{7/2} \rightarrow {}^8S_{7/2}$	$42^\circ$	12 msec
	294	<i>L, W</i>	$t_{2g} \rightarrow {}^6P_{7/2} \rightarrow {}^8S_{7/2}$	$42^\circ$	12 msec
	313	<i>L, W</i>	${}^6P_{7/2} \rightarrow {}^8S_{7/2}$	$42^\circ$	12 msec
	280–350	<i>B, S</i>	$e_g \rightarrow t_{2g} \rightarrow {}^8S_{7/2}$	0	$< 1$ $\mu\text{sec}$
	350–420	<i>B, M</i>	$t_{2g} \rightarrow {}^8S_{7/2}$	0	$< 1$ $\mu\text{sec}$
	450–600	<i>B, W</i>	PSL	0	$< 1$ $\mu\text{sec}$
$\text{BaFCl:Eu}$	260	<i>L, S</i>	${}^6D_{7/2} \rightarrow {}^6P_{7/2} \rightarrow {}^8S_{7/2}$	$> 50^\circ$	$> 15.8$ msec
	265	<i>L, S</i>	${}^6I_{7/2} \rightarrow {}^6P_{7/2} \rightarrow {}^8S_{7/2}$	$50^\circ$	15.8 msec
	280–350	<i>B, S</i>	$e_g \rightarrow {}^8S_{7/2}$	5.6	(0) ( $< 1$ $\mu\text{sec}$ )
			$e_g \rightarrow {}^6P_{7/2} \rightarrow {}^8S_{7/2}$		(50) (15.8 msec)
	350–420	<i>B, S</i>	$t_{2g} \rightarrow {}^8S_{7/2}$	0	$< 1$ $\mu\text{sec}$
450–600	<i>B, W</i>	PSL	0	$< 1$ $\mu\text{sec}$	
$\text{BaCl}_2\cdot\text{Eu}$	250	<i>L, S</i>	${}^6D_{7/2} \rightarrow {}^6P_{7/2} \rightarrow {}^8S_{7/2}$	$> 50^\circ$	$> 15.8$ msec
	263	<i>L, S</i>	${}^6I_{7/2} \rightarrow {}^6P_{7/2} \rightarrow {}^8S_{7/2}$	$> 50^\circ$	$> 15.8$ msec
	281	<i>L, W</i>	$t_{2g} \rightarrow {}^6P_{7/2} \rightarrow {}^8S_{7/2}$	$40^\circ$	11 msec
	305	<i>L, W</i>	${}^6P_{7/2} \rightarrow {}^8S_{7/2}$	$40^\circ$	11 msec
	270–340	<i>B, S</i>	$e_g \rightarrow t_{2g} \rightarrow {}^8S_{7/2}$	0	$< 1$ $\mu\text{sec}$
	340–400	<i>B, M</i>	$t_{2g} \rightarrow {}^8S_{7/2}$	0	$< 1$ $\mu\text{sec}$

<sup>a</sup>*L*, linear peak; *B*, band peak; *S*, strong; *M* middle; *W*, weak.

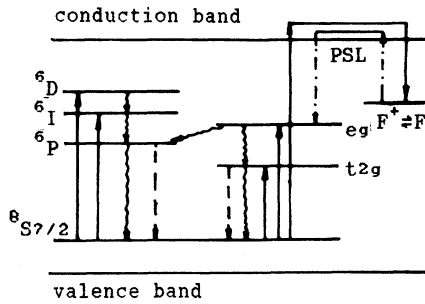


FIG. 6. Energy term scheme of  $\text{BaFCl:Eu}^{2+}$ .  $\longrightarrow$ , the excitation process;  $\rightsquigarrow$ , nonradiative process;  $\dashrightarrow$ , radiative process;  $\dashrightarrow$ , PSL process.

deexcitation process is very small and means this is a fast deexcitation process. This result corresponds to the result of Von Seggern,<sup>10</sup> where the time delay of the PSL process is about 0.8  $\mu\text{sec}$ .

#### B. The PA spectrum of $\text{BaFCl:Eu}^{2+}$

Figure 5 shows the PA amplitude and phase spectrum of  $\text{BaFCl:Eu}^{2+}$ . A strong linear peak with a shoulder is observed at 270–280 nm. It is due to the deexcitation process of  $4f^7 \rightarrow 4f^7$ , see Fig. 6. The phase angle of this linear peak is also larger than  $50^\circ$ . The deexcitation time is calculated as  $>15.8$  msec, the same as that of  $\text{BaFBr:Eu}$ . A band peak is also observed at 290–400 nm. It originates from the deexcitation channel of  $4f^6 5d^1 \rightarrow 4f$  as a very fast process. It also has a shoulder peak at 350–400 nm and it has the same origination as that of  $\text{BaFBr:Eu}^{2+}$ , see Table I. But, in the phase spectrum, there is a small phase shift in the range 290–350 nm. It appears that there are two kinds of deexcitation models of the  $e_g(4f^6 5d^1)$  excited state, such as (i)  $e_g \rightarrow t_{2g} \rightarrow {}^8S_{7/2}$  and (ii)  $e_g \rightarrow {}^6P_{7/2} \rightarrow {}^8S_{7/2}$ , see Fig. 6. Channel (ii) is a slow process and it produces a small phase shift in the deexcitation process of the  $e_g$  state.<sup>16</sup> However, the PSL process is also shown in Fig. 5 at 400–600 nm and it is a very fast process.

#### C. The PA spectrum of $\text{BaCl}_2:\text{Eu}^{2+}$

Figure 7 shows the PA amplitude and phase spectrum of  $\text{BaCl}_2:\text{Eu}^{2+}$ . The spectral properties are also similar to that of  $\text{BaFBr:Eu}^{2+}$  and  $\text{BaFCl:Eu}^{2+}$ , see Table I. But the PSL process is not shown in the PA amplitude spectrum in this material. Based on the weak PA amplitude of band peak in the range 290–400 nm, it is seen that this

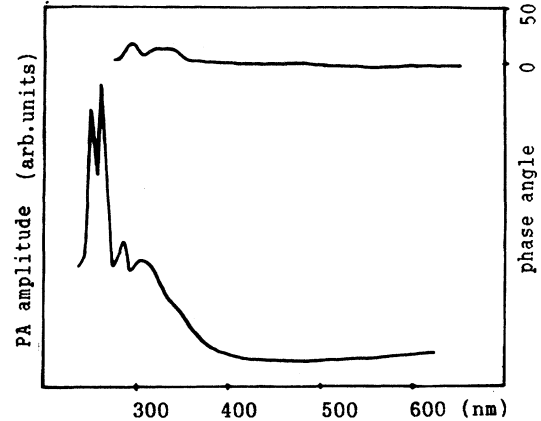


FIG. 7. The PA amplitude and phase spectrum of  $\text{BaCl}_2:\text{Eu}^{2+}$ .

may be due to the high emission efficiency of  $t_{2g}(4f^6 5d^1)$  and the weak nonradiative process.

Comparing Figs. 2, 5, and 7, all the PA amplitudes of these three phosphors have a strong linear peak and a broadband peak. But the PA signal intensities of the band peak are different. It is seen that the emission efficiencies of these three phosphors are different. In our conclusion, the emission efficiencies of the samples in this work have this order:  $\text{BaFCl:Eu}^{2+} < \text{BaFBr:Eu}^{2+} \leq \text{BaCl}_2:\text{Eu}^{2+}$ .

#### IV. CONCLUSIONS

As the PA technique was used, all the deexcitation processes of these three phosphors are assigned and their time delays are calculated. The emission efficiency of the fast deexcitation process  $4f^6 5d^1 \rightarrow 4f^7$  is larger than that of the slow deexcitation process  $4f^7 \rightarrow 4f^7$ . And, the emission efficiencies of the three phosphors are in this order:  $\text{BaFCl:Eu}^{2+} < \text{BaFBr:Eu}^{2+} \leq \text{BaCl}_2:\text{Eu}^{2+}$ . The photostimulated luminescence deexcitation processes are very fast process in these materials and they are corresponding to the Von Seggern's luminescent kinetic process model.

#### ACKNOWLEDGMENTS

I thank the Youth Science Fund of USTC of P.R. China for supporting this work. I also thank Ph.D Don Yi for supporting me with some samples and helpful discussion.

<sup>1</sup>F. Seitz, *Trans. Faraday Soc.* **35**, 74 (1939).

<sup>2</sup>G. F. J. Garlick and A. F. Gibson, *Proc. Phys. Soc.* **60**, 574 (1948).

<sup>3</sup>H. Degenhardt, *Electromedica* **51**, 155 (1983).

<sup>4</sup>K. Takahashi, J. Miyahara, and Y. Shibahara, *J. Electrochem. Soc.* **132**, 1492 (1985).

<sup>5</sup>H. Von Seggern, T. Voigt, and K. Schwarzmittel, *Siemens Res. Develop. Rep.* **17**, 124 (1988).

<sup>6</sup>Y. Iwabuchi, C. Umamoto, K. Takahashi, and S. Shionoya, *J. Lumin.* **48&49**, 481 (1991).

<sup>7</sup>M. Sonoda, M. Takano, J. Miyahara, and H. Kato, *Radiology* **148**, 833 (1983).

- <sup>8</sup>J. Miyahara, K. Takahashi, Y. Amemiya, N. Kamiya, and Y. Satow, *Nucl. Instrum. Methods Phys. Res. A* **246**, 572 (1986).
- <sup>9</sup>K. Takahashi, K. Kohda, J. Miyahara, Y. Kanenritsu, K. Am- itani, and S. Shionoya, *J. Lumin.* **31&32**, 266 (1984).
- <sup>10</sup>H. Von Seggern, T. Voigt, W. Knupfer, and G. Lauge, *J. Appl. Phys.* **64**, 1405 (1988).
- <sup>11</sup>L. D. Merkle and R. C. Powell, *Chem. Phys. Lett.* **46**, 303 (1977).
- <sup>12</sup>H. Vargas and L. C. M. Miranda, *Phys. Rep.* **161**, 43 (1988).
- <sup>13</sup>Zhang Yugeng, Li Jianmin, Su Qinde, and Zhao Guiwen, *Spectrochim. Acta* **48A**, 175 (1992).
- <sup>14</sup>T. Ikari, H. Yokoyama, S. Shigetomi, and K. Futagami, *Jpn. J. Appl. Phys.* **29**, 887 (1990).
- <sup>15</sup>A. Rosencwaig, *Photoacoustics and Photoacoustic Spectroscopy* (Wiley, New York, 1980).
- <sup>16</sup>Zhang Yugeng and Zhao Guiwen, *Cryst. Res. Technol.* **28**, 677 (1993).